

## Neutrino trapping in a supernova and the screening of weak neutral currents

C. J. Horowitz\*

*Nuclear Theory Center and Department of Physics, Indiana University, Bloomington, Indiana 47405*

(Received 9 December 1996)

Neutrino-nucleus elastic scattering is reduced in dense matter because of correlations. The static structure factor for a plasma of electrons and ions is calculated from Monte Carlo simulations and parametrized with a least squares fit. Our results imply a large increase in the neutrino mean-free path. This impacts the trapping of neutrinos in a supernova by coherent neutral current interactions. [S0556-2821(97)03508-X]

PACS number(s): 97.60.Bw, 25.30.Pt, 66.10.-x, 95.30.Cq

A (core collapse) supernova radiates large numbers of neutrinos. Indeed, the energy in neutrinos is 100 times greater than that in all other forms of matter [1]. Therefore, supernova models may depend on the details of neutrino interactions in dense matter. In this paper, we calculate how correlations in the medium modify the important neutrino-nucleus elastic scattering cross section. This cross section is large because of coherent scattering from all of the nucleons in a nucleus [2]. However, when the neutrino wavelength is comparable to the interparticle spacing there are also coherent contributions from different nuclei. These can screen the interaction and lead to a large reduction in the cross section. This reduction is so large that we reexamine the important question of how neutrinos are trapped in a supernova.

In the present supernova model, the core of a massive star runs out of nuclear fuel and collapses [3]. This core is composed of a dense plasma of electrons and nuclei. As the density reaches  $10^{11}$  to  $10^{12}$  g/cm<sup>3</sup> the medium starts to become opaque to neutrinos. The neutrino opacity is thought to be dominated by neutrino-nucleus elastic scattering (as long as a significant fraction of the matter is in nuclei). This opacity ensures that neutrino transport involves diffusion (rather than free streaming). The diffusion time can become long compared to the dynamical time scale, thus trapping neutrinos and their lepton number.

The neutrino-nucleus elastic cross section in free space is [4]

$$d\sigma_0/d\Omega = \frac{G^2 C^2 E_\nu^2 (1 + \cos\theta)}{4\pi^2}, \quad (1)$$

with  $G$  the Fermi constant,  $E_\nu$  the neutrino energy,  $\theta$  the scattering angle, and the total weak charge  $C$  of a nucleus of charge  $Z$  and neutron number  $N$  is

$$C = -2Z\sin^2\Theta_W + (Z - N)/2. \quad (2)$$

(We use a Weinberg angle of  $\sin^2\Theta_W = 0.223$ .) In a dense plasma this cross section is modified by electron [5,6] and ion [7,6] screening. Imagine a single impurity ion in a dense plasma. Extra electrons will be attracted to the impurity. Since these electrons have weak interactions they screen both the electromagnetic and weak charge of the ion. However,

the very dense relativistic electron gas is quite rigid because of the large Fermi momentum. This somewhat limits the effect of electron screening (see below).

Other ions can also screen the impurity by creating a small hole in the ion distribution. At temperatures of order 1 MeV, the ions are essentially classical and their screening is not impeded by a large Fermi energy. Itoh [7] has calculated ion screening in a long wavelength approximation. This is only valid for low neutrino energies. Bowers and Wilson [8] give a better approximation. Ichimaru [11] has calculated screening for a pure one-component plasma. This can be applied to ion screening if the electrons are neglected. Here, we calculate both electron and ion screening with an essentially exact Monte Carlo simulation.

We calculate the total screening for a broad range of densities and determine its impact on the neutrino mean-free path. We provide a parametrization of our results. This allows the incorporation of screening into neutrino transport codes.

Ion screening is included by multiplying Eq. (1) by the static structure factor  $S_q$  of the ions [9] and electron screening by a factor  $R_e^0$ :

$$d\sigma/d\Omega = d\sigma_0/d\Omega S_q R_e^0. \quad (3)$$

Here,  $q$  is the momentum transfer and  $d\sigma/d\Omega$  the effective cross section in the medium. We discuss  $S_q$  below.

The transport cross section is the angle integral of Eq. (3) with a factor of  $(1 - \cos\theta)$ :

$$\sigma^t = \int d\sigma/d\Omega (1 - \cos\theta) d\Omega = \sigma_0^t \langle S \rangle R_e. \quad (4)$$

The free transport cross section is,  $\sigma_0^t = \frac{2}{3} G^2 C^2 E_\nu^2 / \pi$ ,  $\langle S \rangle$  is the angle average of  $S_q$ , and the angle-averaged electron screening factor  $R_e$  is discussed below, see Eq. (19):

$$\langle S(E_\nu, \rho, T) \rangle = \frac{3}{4} \int_{-1}^1 d\cos\theta (1 + \cos\theta)(1 - \cos\theta) S_q(\theta). \quad (5)$$

Here,  $(1 + \cos\theta)$  is from the angular dependence of the free cross section and  $q(\theta)^2 = 2E_\nu^2(1 - \cos\theta)$ . Thus, ion screening can be incorporated into neutrino transport codes by multi-

\*Electronic address: Charlie@iucf.indiana.edu

TABLE I. Parameters  $\beta_{ij}$  from a least squares fit of the angle-averaged static structure factor  $\langle S \rangle$ , see text.

Coeff.	$j=1$	2	3	4
$\beta_{3j}$	-7.362056	0.5371365	-0.1078845	$4.189612 \times 10^{-3}$
$\beta_{4j}$	3.4489581	-0.40251656	$9.0877878 \times 10^{-2}$	$-3.4353581 \times 10^{-3}$
$\beta_{5j}$	-0.74128645	0.11019855	$-2.5359361 \times 10^{-2}$	$9.0487744 \times 10^{-4}$
$\beta_{6j}$	$5.9573285 \times 10^{-2}$	$-1.0186552 \times 10^{-2}$	$2.2791369 \times 10^{-3}$	$-7.4614597 \times 10^{-5}$

plying the existing interactions by the factor  $\langle S \rangle$ .<sup>1</sup> This depends on the density, temperature and neutrino energy. The transport mean-free path  $\lambda$  then follows,  $\lambda = 1/(n\sigma^t)$ , with  $n$  the number density of ions.

The static structure factor  $S_q$  is determined from a Monte Carlo simulation [10] of the radial distribution function  $g(r)$  [11]. This gives the probability to find another ion a distance  $r$  from a given ion and is calculated by histogramming the relative distances in the simulation [10]:

$$S_q = 1 + n \int d^3r e^{-iq \cdot r} [g(r) - 1]. \quad (6)$$

Equations (5) and (6) yield a simple integral for  $\langle S \rangle$ :

$$\langle S \rangle = 1 + \frac{4\pi n}{E_v^2} \int_0^\infty dr f(2E_v r) [g(r) - 1], \quad (7)$$

with

$$f(x) = 72(\cos x + x \sin x - 1)/x^4 - 6(5 \cos x + x \sin x + 1)/x^2. \quad (8)$$

The classical canonical partition function is simulated using  $N_i \approx 1000$  ions in a box of volume  $V = N_i/n$  with periodic boundary conditions. The ions interact via screened Coulomb potentials:

$$v(r) = \frac{Z^2 e^2}{4\pi r} e^{-r/\lambda_e}. \quad (9)$$

Here,  $\lambda_e = \pi/(ek_F)$  describes the electron screening of the ion-ion interaction [12]. Note, this Yukawa approximation can be replaced by a more accurate description at high momentum transfers. However, we are primarily interested in momentum transfers  $q$  much less than the Fermi momentum  $q \ll k_F$ . Therefore, Eq. (9) should be adequate for our purposes.

The system is warmed up for about 200 Metropolis sweeps starting from either a simple cubic lattice or a uniform distribution. Statistics are then accumulated using 400 configurations each of which is separated by five sweeps. This yields  $S_q$  with a typical statistical accuracy of  $(2-3) \times 10^{-3}$ . These results are close to  $S_q$  for a pure one-component plasma [13].

We parametrize our Monte Carlo results for  $\langle S \rangle$  as a function of two dimensionless variables. It is a strong function of

$$\bar{E} = E_v a / \hbar c, \quad (10)$$

(hereafter,  $\hbar c = 1$ ). Here, the ion sphere radius  $a$  measures the average distance between ions [11]:

$$a = [3/(4\pi n)]^{1/3}. \quad (11)$$

Next,  $\langle S \rangle$  is a weak function of  $\Gamma$  which characterizes the strength of the interaction. This is the ratio of a typical Coulomb potential to the thermal energy  $kT$  [11]:

$$\Gamma = \frac{Z^2 e^2}{4\pi a k T}, \quad (12)$$

(with  $e^2 = 4\pi\alpha \approx 0.0917$ ). In general,  $\langle S \rangle$  is a function of the density and temperature separately. However, if one ignores the relatively small effect of the screening length  $\lambda_e$  in Eq. (9) then  $\langle S \rangle$  only depends on  $\Gamma$  (and  $\bar{E}$ ). We have performed simulations for a pure  $^{56}\text{Fe}$  plasma at  $kT = 1$  MeV. We scale our results to other compositions and temperatures by calculating the appropriate  $\Gamma$ .

A least squares fit of our Monte Carlo results valid for all  $E_v$  and  $1 < \Gamma < 150$  is carried out. This fit is based on simulations for 12 values of  $\Gamma$  between 0.87 and 151.8. For a temperature of 1 MeV this corresponds to  $^{56}\text{Fe}$  densities from  $2 \times 10^7$  to  $9 \times 10^{13}$  g/cm<sup>3</sup>. We approximate  $\langle S \rangle$  as a power series in both  $\bar{E}$  and  $\Gamma$ :

$$\langle S(\bar{E}, \Gamma) \rangle = 1 \left/ \left[ 1 + \exp\left(-\sum_{i=0}^6 \beta_i(\Gamma) \bar{E}^i\right) \right] \right. \quad (13)$$

for

$$\bar{E} < E^*(\Gamma) = 3 + 4\Gamma^{1/2}. \quad (14)$$

While for  $\bar{E} > E^*$ , we assume

$$\langle S(\bar{E}, \Gamma) \rangle = 1. \quad (15)$$

The coefficient functions  $\beta_i(\Gamma)$ , for  $i=3, 4, 5$ , and 6 are expanded in a power series in  $\Gamma^{1/2}$ :

$$\beta_i(\Gamma) = \beta_{i1} + \beta_{i2}\Gamma^{1/2} + \beta_{i3}\Gamma + \beta_{i4}\Gamma^{3/2}. \quad (16)$$

The coefficients  $\beta_{ij}$  are collected in Table I. Finite-size effects contaminate the Monte Carlo results for small  $\bar{E}$ . Therefore, we use the random phase approximation (RPA) results for  $\beta_0$ :

$$\beta_0 = \ln[0.300/(0.300 + 3\Gamma)], \quad (17)$$

$\beta_1 = 0$ , and  $\beta_2 = 20/3$ .

<sup>1</sup>Note, Eqs. (1) and (4) have ignored axial-vector current contributions to the cross section. These may be significant when  $\langle S \rangle$  is very small.

The error in the fit is typically less than 0.01. Although, for very large  $\Gamma$ ,  $\langle S \rangle$  oscillates around 1 at large  $\bar{E}$ . This oscillation is not reproduced by our fit and can lead to an error as large as 0.05. However, this only occurs at very high densities and is expected to have negligible impact on the dynamics. Again, the fit is valid for all neutrino energies and  $1 < \Gamma < 150$ . For smaller  $\Gamma$  a good estimate is provided by simply setting  $\Gamma = 1$ . (Note, here  $\langle S \rangle$  is only important at very small neutrino energies.) Likewise, for  $\Gamma > 150$  a reasonable estimate is provided by setting  $\Gamma = 150$  (as long as the system is in the liquid phase). A solid is expected to form for  $\Gamma \approx 180$  [14]. This may be relevant for models of type Ia supernovas [15]. The very interesting problem of ‘‘Bragg diffraction’’ of neutrinos in a radioactive crystal remains to be investigated. Neutrino wavelengths can be comparable to the lattice spacing.

We use this fit for  $\langle S \rangle$  to calculate the mean-free path of a neutrino in a plasma of ions, neutrons, and electrons. For example, Cooperstein and Wambach [16] modeled matter at  $10^{12} \text{ g/cm}^3$  as consisting of  $X_n = 6\%$  free neutrons and 94% nuclei of average charge  $Z \approx 37$  and average mass  $A \approx 97$  at a temperature of 1.5 MeV. This is appropriate for the collapse phase of a supernova. We use this composition in calculating the mean-free path. For simplicity, the composition and temperature are assumed not to change with density and we ignore the strong interactions between ions and/or neutrons.

The transport mean-free path  $\lambda$  is assumed dominated by elastic scattering off of nuclei and neutrons [17]:

$$\lambda = \frac{15 \text{ km}}{\rho_{12}} \left( \frac{10 \text{ MeV}}{E_\nu} \right)^2 \times \left[ (1 - X_n) \frac{C^2}{A} \langle S \rangle R_e + X_n (c_v^{n2} + 5c_a^{n2}) \right]^{-1}. \quad (18)$$

Here,  $\rho_{12}$  is the density in units of  $10^{12} \text{ g/cm}^3$ , the weak couplings of a neutron are  $c_v^n = -1/2$ ,  $c_a^n = -g_A/2$  [18], and  $R_e$  is the additional correction factor that describes electron screening. This is calculated in Ref. [6]. Here, we approximate it as [19] [see below Eq. (9)],

$$R_e \approx \left[ 1 + \left( \frac{c_v^e Z}{C} \right) \frac{1}{1 + 2.0 E_\nu^2 \lambda_e^2} \right]^2. \quad (19)$$

The factor  $2E_\nu^2 \approx \langle q^2 \rangle$  represents the average momentum transfer squared. In the absence of ion screening, this would be  $\frac{4}{3} E_\nu^2$ , given the  $1 + \cos\Theta$  angular distribution of Eq. (1). However, ion screening increases the average momentum transfer and thus somewhat decreases the effect of electron screening.

Each ion has an electron cloud around it. Electron neutrinos or antineutrinos couple to this with strength,  $c_v^e = 2 \sin^2 \Theta_W + \frac{1}{2}$ , while muon neutrinos do not see the electron cloud  $c_v^e \approx 0$ . Thus, electron screening is unimportant for  $\mu$  or  $\tau$  neutrinos,  $R_e \approx 1$ .

The mean-free path  $\lambda$  is shown in Fig. 1. Without screening, the mean-free path is very short. This traps neutrinos for densities of about  $\rho_{12} = 0.5$  and above. However, including  $\langle S \rangle$  leads to a dramatic increase in  $\lambda$  and to a large change in

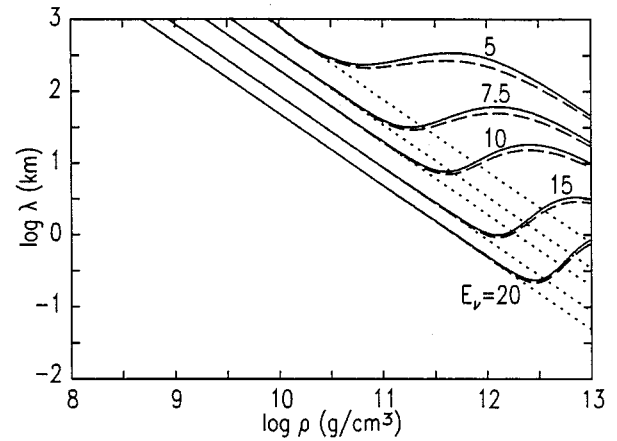


FIG. 1. Neutrino transport mean-free path vs density. The solid lines include both ion  $\langle S \rangle \neq 1$  and electron  $R_e \neq 1$  screening and are appropriate for  $\nu_e$ ,  $\bar{\nu}_e$  while the dashed lines for  $\nu_\mu$  neglect electron screening  $R_e = 1$ . Finally, the dotted lines neglect all screening  $\langle S \rangle = R_e = 1$ . Top to bottom, the curves are for neutrino energies of  $E_\nu = 5, 7.5, 10, 15,$  and  $20$  MeV. The logarithm is to base 10.

its density dependence. The rapid decrease of  $\langle S \rangle$  with density can lead to a  $\lambda$  which actually *increases* with density. Over a range of densities,  $\lambda$  for  $E_\nu = 10$  MeV is greater than 10 km. This is much larger than the unscreened  $\lambda$  ( $\approx 0.4$  km at  $\rho_{12} = 5$ ).

Finally, electron screening causes  $\lambda$  for a  $\nu_e$  to be about 15% *larger* than that for a  $\nu_\mu$ . This is because the extra charged current interactions of the  $\nu_e$  interfere destructively with the dominant neutral currents. Therefore, the total cross section for a  $\nu_e$  is smaller and the mean-free path longer than that for a  $\nu_\mu$ .

Screening effects are even more important for lower  $E_\nu$ . For example, at 5 MeV,  $\lambda$  is greater than 45 km even at  $\rho_{12} = 10$ . This is larger than the size of the dense system ( $\approx 30$  km) so a neutrino sphere may not form at all (for this energy).

Figure 1 shows that  $\lambda$  is larger than the size of the system for  $E_\nu$  less than or equal to about 7.5 MeV. For  $E_\nu$  between 7.5 and about 10 MeV, the relatively large  $\lambda$  will allow neutrinos to diffuse out of the system (in about a msec or less). These are the main results of this paper.

However, at  $E_\nu = 20$  MeV (or above), screening is reduced and the overall  $1/E^2$  scale of  $\lambda$  is smaller so that the mean-free path is significantly shorter. The mean-free path is not very sensitive to temperature (as long as there are no large changes in composition). Changing  $T$  leads to a change in  $\Gamma$ , see Eq. (12). However,  $\langle S \rangle$  is not a strong function of  $\Gamma$ .<sup>2</sup> Likewise,  $\langle S \rangle$  is not very sensitive to the average  $Z$  of the material. Changes in the average  $A$  change  $a$  in Eq. (10) and the overall factor  $C^2/A$  in Eq. (18). Thus,  $\lambda$  decreases with increasing  $A$ .

Screening effects will be all but absent after the supernova shock wave dissociates nuclei. Then,  $\lambda$  will be rela-

<sup>2</sup>Except for very low neutrino energies where  $\langle S \rangle$  is small and goes like  $1/\Gamma$ . However, here the mean-free path is dominated by the neutrons.

tively short because of scattering from large numbers of nearly free neutrons and protons. Thus, the neutrino opacity is small (because of screening) before the shock wave and large afterwards. Perhaps, the situation is not unlike the photon opacity of the universe being large before and small after recombination.

Neutrino electron scattering (NES) is unimportant for the transport mean-free path (we find this to be true even when  $\langle S \rangle$  is small). However, NES is important for the energy loss. Therefore, we note the effects of screening on NES. This was calculated in Ref. [6] and can be included by multiplying the NES cross section of a relativistic free Fermi gas by a factor  $R_{ee}$  in analogy to Eq. (4). Note, ion screening is assumed to be unimportant, since the response of the slow ions is small at high excitation energies.

We approximate  $R_{ee}$ , as deduced from the full calculations in Ref. [6], by

$$R_{ee} = \frac{1}{c_v^{e2} + c_a^{e2}} \left[ \frac{c_v^{e2}}{1 + \frac{3}{4} E_\nu^{-2} \lambda_e^{-2}} + c_a^{e2} \right]. \quad (20)$$

Here, vector currents are screened and axial-vector currents (largely) unscreened. For electron neutrinos ( $c_a^e = -1/2$ ),

$$R_{ee} \approx 0.782 [1 + 18.5 (Y_e \rho_{12})^{2/3} E_\nu^{-2}]^{-1} + 0.218, \quad (21)$$

with  $E_\nu$  in MeV and  $Y_e$  is the number of electrons per baryon, while  $R_{ee} \approx 1$  for  $\nu_\mu$  and  $\nu_\tau$ . In practice, screening of NES is important only for low energies and thus may not impact the dynamics significantly.

For completeness, we give a simple approximation to the (unscreened) NES cross section of a relativistic Fermi gas which is valid in the limit  $E_\nu \ll k_F$ :

$$\sigma = \frac{G^2 (c_v^{e2} + c_a^{e2}) E_\nu^3}{5 \pi k_F}. \quad (22)$$

The factor of  $E_\nu/k_F$  is from Pauli blocking since only electrons within  $E_\nu$  of the Fermi surface can be ejected by the neutrino. In this limit ( $E_\nu \ll k_F$ ), the average energy lost by the neutrino per collision is  $E_\nu/3$ . We emphasize this simple formula is to be used only in the qualitative discussion below. It is not quantitative because  $E_\nu$  is often less than  $k_F$  but not much less. For example, Eq. (22) is off by about 10% at  $E_\nu = 10$ ,  $k_F = 50$  MeV.

We now discuss the implications of screening on supernova simulations. Screening will allow more neutrinos to escape, thus lowering the lepton fraction  $Y_l$  (number of electrons and neutrinos per baryon) of the core. Simulations are very sensitive to  $Y_l$  because there is a delicate balance between Fermi pressure which depends on  $Y_l$ , and gravity which is independent of  $Y_l$ . A lower  $Y_l$  will weaken the shock and cause it to stall at a smaller radius [21].

Thus, it is important to determine when and how neutrinos are trapped in a supernova. Previously, it was thought neutrinos are trapped at a density near  $\rho_{12} \approx 0.5$  when the diffusion time scale to make it out of the dense core becomes long compared to the dynamical time scale of the collapse. However, when screening is included, the *escape time scale*

is *comparable* to the dynamical time scale. Thus, the concept of a trapping density is not so straightforward.

Note, screening does not simply increase the trapping density. In fact, increasing the density can make matters worse (and allow more neutrinos to escape). This is because screening increases rapidly with density so that the mean-free path *increases* with density.

During collapse, neutrinos are produced at relatively high energies (of order 5/6 of the electron Fermi energy) from electron capture. At these energies of 20 MeV and above, neutrinos are trapped even with screening. However, neutrino electron scattering can rapidly reduce these high energies. Therefore, the escape time scale is the appropriate combination of the time to down scatter in energy from NES and the time to escape by diffusion. For example, a 20 MeV (or higher) electron neutrino produced at  $\rho_{12} = 5$  can have its energy reduced to about 10 MeV in a time of order 1/3 msec by electron scattering. The neutrino can then diffuse out of the core in about a msec. Alternatively, the neutrino's energy can be reduced to 7.5 MeV (in about a msec) and then directly escape. Note, the dynamical time scale for collapse is also about a msec (near  $\rho_{12} = 1$ ).

Since the escape and collapse time scales are comparable, neutrino trapping during in-fall is a somewhat delicate issue. If a supernova only produced a few neutrinos then a significant fraction of these would escape. However, it produces so many that they all cannot get out at once. Thus, Pauli blocking of the low energy neutrino phase space may be important for trapping. High energy neutrinos are trapped even with screening. The role of screening is to broaden the window of low energy states from very low energies to  $E_\nu \approx 10$  MeV and below through which neutrinos can escape. This should lead to a significant but not gigantic reduction in the  $Y_l$  of the core.

Another implication of screening is an increase in the neutrino luminosity because of the increased diffusion. Indeed, Lattimer and Burrows find that ion screening increases the luminosity in the cooling phase of proto-neutron star formation [20]. To our knowledge, no previous simulations have included both ion and electron screening. The modest ( $\approx 15\%$ ) effect of electron screening, although smaller than ion screening, could still lead to a significant increase in the luminosity. This may enhance the neutrino transport of energy to the shock. Note, screening has almost no effect on the opacity of low density matter or of the dissociated material after shock passage. Thus, screening should not interfere with the ability of material near the shock to absorb energy from neutrinos.

Finally, screening may impact the neutrino spectrum. One could guess that a reduction in opacity hardens the spectrum by allowing one to "see" further into the hot core. However, the strong energy dependence of screening probably more than compensates for this leading to a net softening of the spectrum. Electron screening, since it is important for  $\nu_e$ ,  $\bar{\nu}_e$  only, could effect the difference between the  $\nu_e$  and  $\nu_\mu$  spectra.

We have calculated the effects of electron and ion screening on neutrino-nucleus elastic scattering. Our Monte Carlo results for the angle average of the static structure factor have been fitted to an analytic formula. This allows the in-

clusion of screening in simulations. We find that the mean-free path of a 10 MeV (or lower) neutrino is greatly increased. This causes the collapse time scale and the neutrino escape time scale to be *comparable*. This may complicate neutrino trapping during the in-fall phase of a supernova.

We thank the Institut für Theoretische Kernphysik in Bonn for their kind hospitality where most of this work was done. This research was supported in part by the U.S. Department of Energy under Grant No. DE-FG02-87ER-40365 and by the Deutsche Forschungsgemeinschaft.

- 
- [1] A. Burrows, *Annu. Rev. Nucl. Part. Sci.* **40**, 181 (1990).  
 [2] D. Z. Freedman, D. N. Schramm, and D. L. Tubbs, *Annu. Rev. Nucl. Sci.* **27**, 167 (1977).  
 [3] H. A. Bethe, *Annu. Rev. Nucl. Part. Sci.* **38**, 1 (1988); H. A. Bethe, G. E. Brown, J. Applegate, and J. M. Lattimer, *Nucl. Phys.* **A324**, 487 (1979); S. W. Bruenn, *Astrophys. J.* **340**, 955 (1989); **341**, 385 (1989); M. Herant, W. Benz, W. P. Hix, C. L. Fryer, and S. A. Colgate, *ibid.* **435**, 339 (1994); A. Burrows, J. Hayes, and B. A. Fryxell, *ibid.* **450**, 830 (1995).  
 [4] A. Drukier and L. Stodolsky, *Phys. Rev. D* **30**, 2295 (1984).  
 [5] L. B. Leinson, V. N. Oraevsky, and V. B. Semikoz, *Phys. Lett. B* **209**, 80 (1988).  
 [6] C. J. Horowitz and K. Wehrberger, *Phys. Rev. Lett.* **66**, 272 (1991).  
 [7] N. Itoh, *Prog. Theor. Phys.* **54**, 1580 (1975).  
 [8] R. L. Bowers and J. R. Wilson, *Astrophys. J. Suppl. Ser.* **50**, 115 (1982).  
 [9] See, for example, P. Nozieres, *Theory of Interacting Fermi Systems* (Benjamin, N.Y., 1964), p. 53.  
 [10] See, for example, W. L. Mcmillan, *Phys. Rev.* **138**, A442 (1965).  
 [11] S. Ichimaru, *Rev. Mod. Phys.* **54**, 1017 (1982); S. Ichimaru, H. Iyetomi, and S. Tanaka, *Phys. Rep.* **149**, 91 (1987).  
 [12] A. L. Fetter and J. D. Walecka, *Quantum Theory of Many-Particle Systems* (McGraw-Hill, New York, 1971), p. 175.  
 [13] S. Galam and J. P. Hansen, *Phys. Rev. A* **14**, 816 (1976).  
 [14] S. Ogata and S. Ichimaru, *Phys. Rev. A* **36**, 5451 (1987).  
 [15] R. Canal in *Supernovae*, edited by S. Bludman, R. Mochkovitch, and J. Zinn-Justin (North Holland, Amsterdam, 1994), p. 155.  
 [16] J. Cooperstein and J. K. Wambach, *Nucl. Phys.* **A420**, 591 (1984).  
 [17] G. E. Brown, H. A. Bethe, and G. Baym, *Nucl. Phys.* **A375**, 481 (1982).  
 [18] C. J. Horowitz and K. Wehrberger, *Nucl. Phys.* **A531**, 665 (1991).  
 [19] C. J. Horowitz (unpublished).  
 [20] J. M. Lattimer and A. Burrows, in *Proceedings of the ESO/EPIC Workshop, 1991*, edited by I. J. Danziger and K. Kjar, *Eso Workshop and Conference Proceedings No. 37* (unpublished), p. 69.  
 [21] S. W. Bruenn and W. C. Haxton, *Astrophys. J.* **376**, 678 (1991).